Atmospheric Environment 222 (2020) 117102

Contents lists available at ScienceDirect

Atmospheric Environment

journal homepage: http://www.elsevier.com/locate/atmosenv

Seasonal variation of amine-containing particles in urban Guangzhou, China

Xiufeng Lian [a,b], Guohua Zhang [a,*], Qinhao Lin [a], Fengxian Liu [c], Long Peng [a,b], Yuxiang Yang [a,b], Yuzhen Fu [a,b], Feng Jiang [a,b], Xinhui Bi [a,**], Duohong Chen [d], Xinming Wang [a], Ping'an Peng [a], Guoying Sheng [a]

[a] State Key Laboratory of Organic Geochemistry and Guangdong Provincial Key Laboratory of Environmental Protection and Resources Utilization, Guangzhou Institute of Geochemistry, Chinese Academy of Sciences, Guangzhou, 510640, PR China
[b] University of Chinese Academy of Sciences, Beijing, 100049, PR China
[c] Taiyuan University of Technology, Taiyuan, 030024, PR China
[d] Guangdong Environmental Monitoring Center, Guangzhou, 510308, PR China

HIGHLIGHTS

- The number fraction of amine-containing particles in spring/summer is higher.
- Trimethylamine and diethylamine distribute differently over particle types.
- Compared with trimethylamine, diethylamine is associated with more sulfate.
- A large fraction of trimethylamine is observed to be oxidized mainly at night.

ARTICLE INFO

Keywords:
Amine
Seasonal variation
Mixing state
TMA
DEA

ABSTRACT

Amines are ubiquitous in the environment and pose potential impacts on atmospheric chemistry; however, their seasonal variations and atmospheric processes remain unclear. In this study, a single-particle aerosol mass spectrometer is employed to investigate the seasonal variations of amine-containing particles as well as the oxidation of trimethylamine (TMA) in the urban region of Guangzhou, China. Number fractions of the amine-containing particles exhibit distinct seasonal variations, with higher fractions in spring and summer. Four amines, namely, TMA, diethylamine (DEA), dipropylamine, and tripropylamine are observed over all the seasons. DEA and TMA are the most dominant and account for approximately 90% of all these amine-containing particles. They are mainly clustered into eight types, comprised of internally mixed organics and elemental carbon (OCEC), OC–K, EC, Metal–rich, Dust, NaK–EC, Amine–rich, and high molecular weight organic compounds. DEA and TMA distribute differently over particle types and exhibit a distinct mixing state because of their different physicochemical properties. Compared with TMA, DEA is associated with more sulfate. The possible oxidation of TMA is also investigated, and the results indicate the potential contribution of aqueous oxidation or NO_3 radical oxidation to the formation of TMA oxide. Overall, the results improve the comprehension of the formation and evolution processes of amines in atmospheric environment.

1. Introduction

As one of the most important classes of nitrogen-containing organic compounds, amines pose a potential impact on atmospheric chemistry, global N cycle, and climate system. Amines are emitted from numerous natural and anthropogenic sources, such as animal husbandry, marine sources, biomass burning, industrial processes, and vehicle exhaust (Facchini et al., 2008; Rappert and Müller, 2005; Rui et al., 2009; Youn et al., 2015). Globally, the concentration of gaseous amines is one or two orders of magnitude lower than that of ammonia depending on location

* Corresponding author.
** Corresponding author.
E-mail addresses: zhanggh@gig.ac.cn (G. Zhang), bixh@gig.ac.cn (X. Bi).

https://doi.org/10.1016/j.atmosenv.2019.117102
Received 28 April 2019; Received in revised form 18 October 2019; Accepted 31 October 2019
Available online 6 November 2019

(Ge et al., 2011a). Theoretical calculations and laboratory studies reveal that amines have an advantage over ammonia in neutralizing acidic aerosol (Bzdek et al., 2010), and they perform a pivotal function in new particle formation (Almeida et al., 2013). Recent studies indicate that amines potentially contribute to the formation of brown carbon, and thus have a remarkable influence on direct radiative forcing (De Haan et al., 2017; Powelson et al., 2014).

Gaseous amines can be combined with inorganic and organic acids to form aminium salts (Angelino et al., 2001; Murphy et al., 2007). They can also react with ozone (O_3), hydroxyl radical (OH), or nitro radical (NO_3) to form secondary organic aerosols (Murphy et al., 2007; Price et al., 2014; Qiu and Zhang, 2013; Silva et al., 2008; Tang et al., 2013). Aminium salts exhibit a potential influence on the morphology, density, volatility, absorbability, hygroscopicity, and cloud condensation activities (Qiu and Zhang, 2013). Recently, the application of single particle mass spectrometry (SPMS) with a high time resolution is a great aid to comprehend the mixing state and evolution of amine-containing particles in the atmosphere. Sorooshian et al. (2007) and Huang et al. (2012) showed the presence of diethylamine (DEA) nitrate and sulfate in ambient aerosols. Pratt et al. (2009) described a strong seasonal dependence of aminium salts. The single scattering albedo for aldehyde-amine mixtures increases with the methyl substitution of amines (Marrero-Ortiz et al., 2019). The acid–base reactions responsible for the formation of aminium salts in the particle phase, however, have not been fully explored. In addition, reactions between amines and NO_3 radicals are sufficiently fast to compete with acid–base reactions in smog chamber studies (Malloy et al., 2009; Silva et al., 2008). Nevertheless, the oxidation of amines in ambient aerosols has not been explored yet.

Various factors, such as meteorological conditions, particle properties, and atmospheric oxidation capacity affect the partitioning of amines to the particle phase. A number of field studies have demonstrated that a higher relative humidity (RH) significantly enhances the partitioning of gaseous amines (DEA and TMA) to the particle phase (Chen et al., 2019; Liu et al., 2018; Rehbein et al., 2011; Zhang et al., 2012). Theoretical calculation by Ge et al. (2011b) showed that acidic particles have a high tendency to absorb amines from the gas phase, and low temperatures are generally favorable for the formation of aminium salt aerosols. Huang et al. (2012) observed a higher number fraction of amine-containing particles during winter in Shanghai. In contrast, Cheng et al. (2018) reported more amine-containing particles in summer than in winter. This is mainly caused by the higher particulate acidity and/or RH during summer. It is therefore considerably important to further explore the composition, formation, and evolution mechanisms of particle phase amines in the atmosphere.

Guangzhou is the largest city in the Pearl River Delta (PRD) region of China. Abundant amines have been detected in Guangzhou's atmosphere. The concentration of total amines (79.6–140.9 ng m^{-3}) in this region is slightly higher than those in other urban environments (Liu et al., 2017). While the mixing state and evolution of TMA-containing particles has been discussed in foggy episode (Zhang et al., 2012), seasonal variations of amines and their evolution in the atmosphere have not been investigated. In this paper, observations of individual amine-containing particles based on SPMS in urban Guangzhou region are presented. The specific objectives are summarized as follows: 1) to characterize the seasonal variations of amine-containing particles and identify the influencing factors; 2) to investigate the chemical

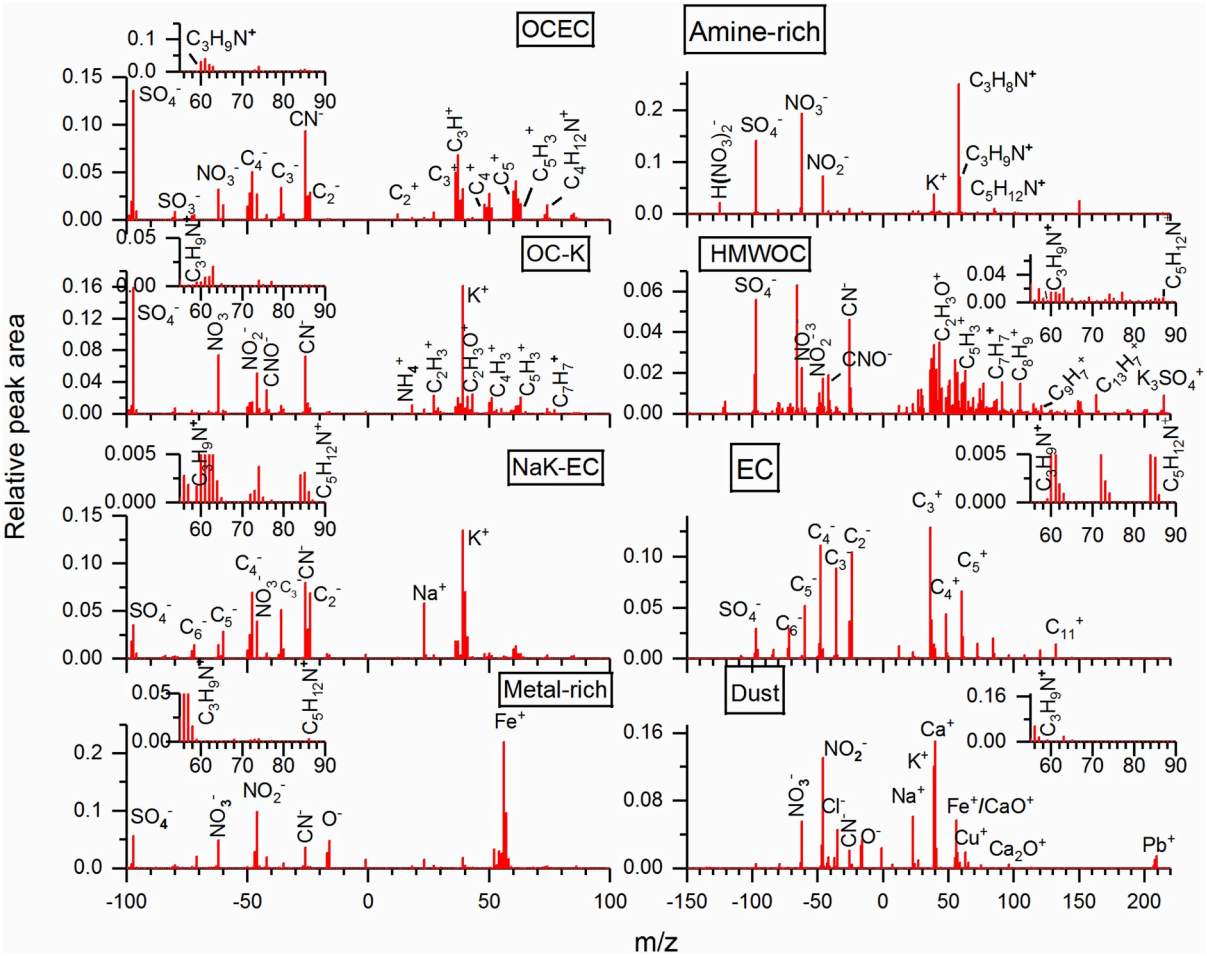

Fig. 1. Average mass spectra of the main amine particle types.

Table 1
Summary of number and number fraction (Nf) of detected amine-containing particles and fragments over the sampling seasons.

Species		Spring		Summer		Fall		Winter	
	Marker ion	Number	Nf(%)[b]	Number	Nf(%)	Number	Nf(%)	Number	Nf(%)
All particles[a]		675 713		160 742		1 870 733		5 265 859	
Total amines		30 076	4.5	46 276	28.8	22 863	1.2	40 526	0.77
m/z 59	$[(CH_3)_3N]^+$	4932	0.73	9192	5.7	9973	0.53	24 289	0.46
m/z 86	$[(C_2H_5)_2NCH_2]^+$	25 080	3.7	37 670	23.4	11 246	0.6	13 271	0.25
m/z 102	$[(C_3H_7)_2NH_2]^+$	1186	0.18	2810	1.7	646	0.035	2338	0.044
m/z 114	$[(C_3H_7)_2NCH_2]^+$	252	0.037	1283	0.8	1521	0.081	3212	0.061
m/z 143	$[(C_3H_7)_3N]^+$	120	0.018	597	0.37	511	0.027	269	0.0051

[a] All particles have both positive and negative spectra.
[b] Number fraction (Nf) is calculated by dividing the number of amine by the number of particles.

compositions and mixing state of amine-containing particles; 3) to discuss the atmospheric evolution of amines in particles.

2. Experiments

2.1. Sampling

The sampling site (23.15° N, 113.37° E) is located at Guangzhou Institute of Geochemistry, Chinese Academy of Sciences. It is a typical urban site, ~100 m from the major traffic zone and 2 km away from the city center (Bi et al., 2011). The sampling inlet is ~2 m above the roof of a nine-story building (~30 m). The sampling periods cover spring (March 9–April 8, 2014), summer (June 16–July 9, 2014), fall (September 15–October 16, 2014), and winter (December 15, 2014–January 15, 2015). The samples collected between September 27 and October 18, 2013 are employed to study TMA oxidation processes. In these samples, the number of TMAO-containing particles detected is larger than those detected in 2014. The local meteorological data that include RH, temperature (*T*), wind speed (WS), wind direction (WD), and concentrations of nitrogen oxide (NO_x), sulfur dioxide (SO_2), O_3, and $PM_{2.5}$ are provided by the Guangdong Environmental Monitoring Center (Table S1).

2.2. Instrumentation

Sizes and chemical compositions of individual particles are measured using a commercial single particle aerosol mass spectrometer (SPAMS, Hexin Analytical Instrument Co., Ltd., Guangzhou, China). The detailed setup and mechanisms involving SPAMS are described elsewhere (Li et al., 2011). The aerosol particles are sampled into an aerodynamic lens through a 0.1-mm critical orifice at a flow rate of 80 mL min^{-1}. They are thereafter aerodynamically sized by two continuous diode Nd:YAG laser beams (532 nm), followed by desorption/ionization using a pulsed laser (266 nm) exactly triggered based on the flight time during sizing. The resulting positive and negative ions are detected by a time-of-flight spectrometer.

2.3. SPAMS data analysis

The information on particle sizes and mass spectra is imported into the MATLAB based YAADA 2.1 toolkit (www.yaada.org) for further analysis. Amine-containing particles are identified by querying m/z 59 $[(CH_3)_3N]^+$, 86 $[(C_2H_5)_2NCH_2]^+$, 102 $[(C_3H_7)_2NH_2]^+$, or 143 $[(C_3H_7)_3N]^+$, which are most probably found in the fragments of the TMA, DEA, DPA and TPA, respectively (Angelino et al., 2001; Healy et al., 2015). The m/z 114 $[(C_3H_7)_2NCH_2]^+$) ion is most probably found in the fragments of DPA or TPA (Angelino et al., 2001; Healy et al., 2015). Querying m/z 46 $[(CH_3)_2NH_2]^+$ and 101$[(C_2H_5)_3N]^+$ is not performed because of interference (with details provided in the Supplement), although they might be produced from amines.

DEA and TMA, which contribute to more than 90% of amine-containing particles over the four seasons, are chosen to explore the of amine-containing particles. Single particle mass spectra are clustered with ART-2a method based on the similarities of mass-to-charge ratio and peak intensity (Song et al., 1999). The parameters used for ART-2a are the vigilance factor at 0.70, learning rate at 0.05 and interactions at 20. Approximately 95% of particles classified by ART-2a are manually classified into five to eight main types. The particle types are as follows: internally mixed organics and elemental carbon (OCEC), OC–K, EC, Metal–rich, Dust, NaK–EC, Amine–rich and high molecular weight organic compounds (HMWOC). The remaining particles are grouped together as "Others."

3. Results and discussion

3.1. Characterization of amine-containing particle types

Fig. 1 depicts the average positive and negative mass spectra of the eight particle types. Compared with other types, the OCEC particles are characterized by OC fragments (m/z 27 $[C_2H_3]^+$, 29 $[C_2H_5]^+$, 37 $[C_3H]^+$, 51 $[C_4H_3]^+$, and 63 $[C_5H_3]^+$), EC fragments (m/z 12 $[C]^+$, 36 $[C_3]^+$, and 60 $[C_5]^+$), and the strongest amines fragments (m/z 74 $[(C_2H_5)_2NH_2]^+$ and 86 $[(C_2H_5)_2NCH_2]^+$). The mass spectral patterns of OC-K particles show a series of OC fragments, strong K^+ (m/z 39 $[K^+]$), and weak EC fragments. The m/z 43 $[C_2H_3O]^+$ in OC–K particles confirms the aging of these particles (Denkenberger et al., 2007). The HMWOC particles are mainly composed of OC fragments and high mass ion peaks in a range of 100–200 (m/z 115 $[C_9H_7]^+$, 128 $[C_{10}H_8]^+$, 152 $[C_{12}H_8]^+$, 163 $[C_{13}H_7]^+$, 165 $[C_{13}H_9]^+$, 189 $[C_{15}H_9]^+$, and 202 $[C_{16}H_9]^+$) (Qin and Prather, 2006; Zhang et al., 2015).

EC particles show a significant number of EC fragments (m/z ±12 $[C]^{+/-}$, ±24 $[C_2]^{+/-}$, ±36 $[C_3]^{+/-}$, ±48 $[C_4]^{+/-}$, and ±60 $[C_5]^{+/-}$, …) with minor peaks of nitrate and sulfate (m/z −97 $[SO_4]^-$). The NaK–EC particles are characterized by the highest peak at m/z 39 $[K]^+$ and a smaller peak at m/z 23 $[Na]^+$ along with EC fragments in the negative spectrum.

The Dust particles are identified as m/z 23 $[Na]^+$, 39 $[K]^+$, 40 $[Ca]^+$, 56 $[CaO/Fe]^+$, and 208 $[Pb]^+$. The negative spectrum is dominated by nitrate, m/z −16 $[O]^-$, and −35/37 $[Cl]^-$. The Metal–rich particles usually contain one or more characteristic peaks of metals (m/z 51 $[V]^+$, 52 $[Cr]^+$, 55 $[Mn]^+$, 56 $[Fe]^+$, and 67 $[VO]^+$) in the positive spectrum, whereas nitrate and sulfate are found in the negative spectrum.

The Amine–rich particles exhibit strong peaks at m/z 58 $[C_3H_8N]^+$, 59 $[(CH_3)_3N]^+$, or 86 $[(C_2H_5)_2NCH_2]^+$ in the positive spectrum. Secondary species that consist of m/z −46 $[NO_2]^-$, −62 $[NO_3]^-$, −97 $[SO_4]^-$, and −125 $[H(NO_3)_3]^-$ are also observed in the Amine–rich type. The ion peak at m/z −125 suggests that these particles are highly acidic (Müller et al., 2009).

3.2. Seasonal variation of amine-containing particles

The number fractions of amines during the sampling periods are summarized in Table 1. 30 076, 46 276, 22 863, and 40 526 amine-containing particles, which account for 4.5%, 28.8%, 1.2%, and 0.8%

Table 2
Pearson correlation coefficients (r) between number fractions of amine-containing particles and meteorological parameters (RH: relative humidity; T: temperature; WS: wind speed), relative particle acidity (relative acidity), and gas pollutants (NO_X; O_3 and SO_2). The relative particle acidity is calculated by dividing the sum of sulfate and nitrate peak areas by the ammonium peak area (Denkenberger et al., 2007; Pratt et al., 2009).

	Spring	Summer	Fall	Winter
RH	0.41[a]	−0.006	0.39[a]	−0.30[a]
T	−0.52[a]	−0.052	−0.13[b]	−0.098
WS	0.024	0.018	0.21[a]	0.007
Acidity	0.14[b]	−0.045	0.38[a]	−0.034
NO_X	0.17[a]	−0.27[a]	0.057	−0.048
O_3	−0.50[a]	0.009	−0.43[a]	0.12[a]
SO_2	0.002	−0.35[a]	−0.042	0.17[a]

[a] Correlation is significant at 0.01 level (two-tailed).
[b] Correlation is significant at 0.05 level (two-tailed).

of all particles, respectively, from spring to winter, are identified. In line with other studies (Cheng et al., 2018; Healy et al., 2015), the contributions from DPA and TPA-containing particles are limited in all seasons.

Many factors, such as RH, T, relative particle acidity, NO_x and SO_2 may affect the variation of particulate amines (Ge et al., 2011b; Qiu and Zhang, 2013), in addition to source strength. Lower T and higher RH promote the gas-solid and gas-aqueous partitioning of amines, respectively, while the relative particle acidity, SO_2 and NO_x concentration directly or indirectly affect the acid–base reaction of amines (Ge et al., 2011b). In the present study, correlation analysis is adopted to distinguish the main factors affecting the variation of amines. The correlation coefficients between the number fractions of amine-containing particles and meteorological parameters, relative particle acidity, and gas pollutants are listed in Table 2. The number fractions of amine-containing particles exhibit positive correlations (spring: $r = 0.41$, $p < 0.01$; fall: $r = 0.39$, $p < 0.01$) with the RH in spring and fall. The number fractions of amine-containing particles showed a negative correlation with T ($r = -0.52$, $p < 0.01$) in spring, and a positive correlation with relative particle acidity ($r = 0.38$, $p < 0.01$) in fall. In summary, low temperature and high RH may promote the distribution of amines into the particle phase during spring, whereas RH and particle acidity perform a more important function in fall.

With a high RH (80 ± 13%) in summer, the number fractions of amine-containing particles show no correlation with RH. Nevertheless, it shows a negative correlation with the concentration of NO_x species ($r = -0.27$, $p < 0.01$) and SO_2 ($r = -0.35$, $p < 0.01$). SO_2 and NO_x species are important precursors of nitric acid (HNO_3) and sulfuric acid (H_2SO_4) in the environment. These acids may further react with amines to generate aminium salts (Ge et al., 2011a; Liu et al., 2018; Pathak et al., 2009; Tao et al., 2012). We therefore speculate that acid–base reaction may be more important than direct dissolution for the formation of particulate amines in summer. Totally, these results show that the number fractions of amine-containing particles are positively correlated with RH in spring and fall, but not in summer and winter. It may indicate that RH was less important than other factors in summer and winter.

The relative number abundance distribution of main amine particle types during each season is shown in Fig. S1. Carbonaceous particle types (OCEC, OC−K, HMWOC, EC, and NaK−EC) are predominant throughout the year. The OCEC type exhibits significant seasonal variations with higher number fractions in spring (30.4%) and summer (28.2%) and lower number fractions in fall (8.1%) and winter (6.8%). More Dust particles are more frequently observed during fall (9.4%) and winter (23.3%), compared with spring (3.9%) and summer (0.2%). The detailed information on the temporal variations of particle types in amine-containing particles is shown in Fig. S2.

It is noteworthy that the distributions of various particle types between DEA and TMA-containing particles distinctly differ. OC–K and OCEC types have the largest number fractions in DEA-containing particles during the four seasons (Fig. 2). The number fractions of other particle types are generally less than 5%. The number fractions of Metal–rich (2.1–12.1%) and Dust (16.0–30.2%) types in TMA-containing particles are higher, however, than those in DEA-containing particles. The number fraction of the OCEC type in TMA-containing particles (0–15.0%) is evidently lower than that in DEA-containing particles (10.0–34.2%). Notably, the HMWOC exhibits a significant number fraction (13.3%) in TMA-containing particles that may be partly generated from the oxidation of TMA (as discussed in Section 3.4).

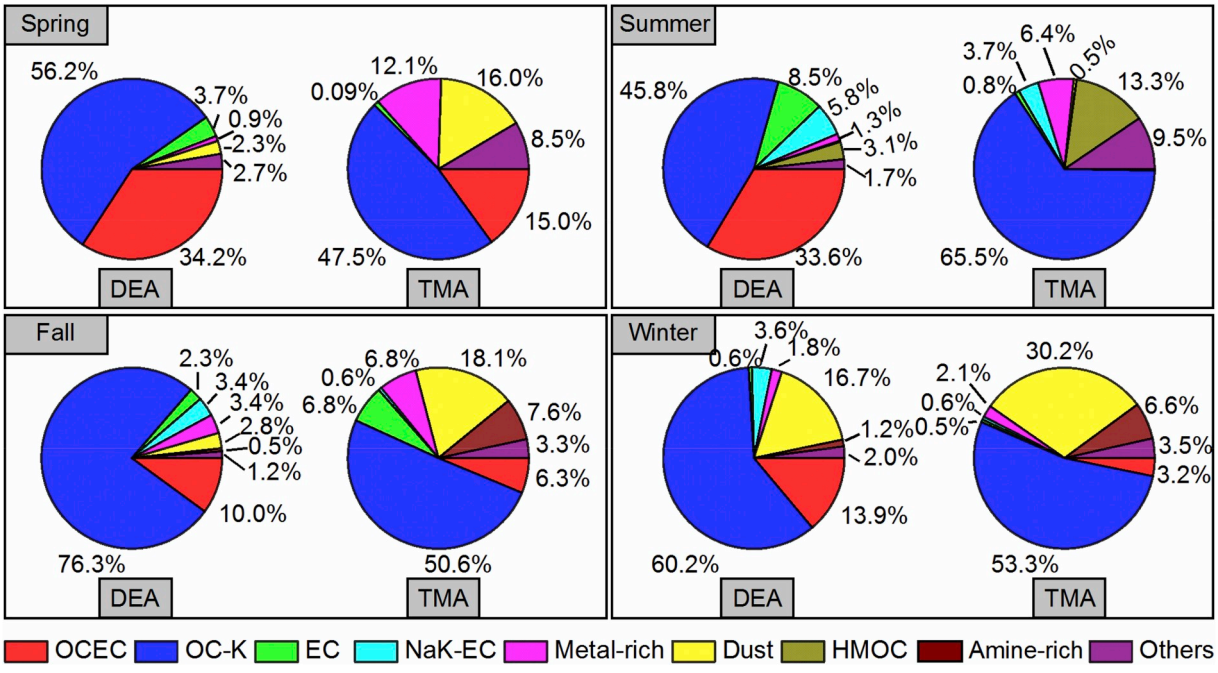

Fig. 2. Number fraction of the main types for DEA- and TMA-containing particles in every season.

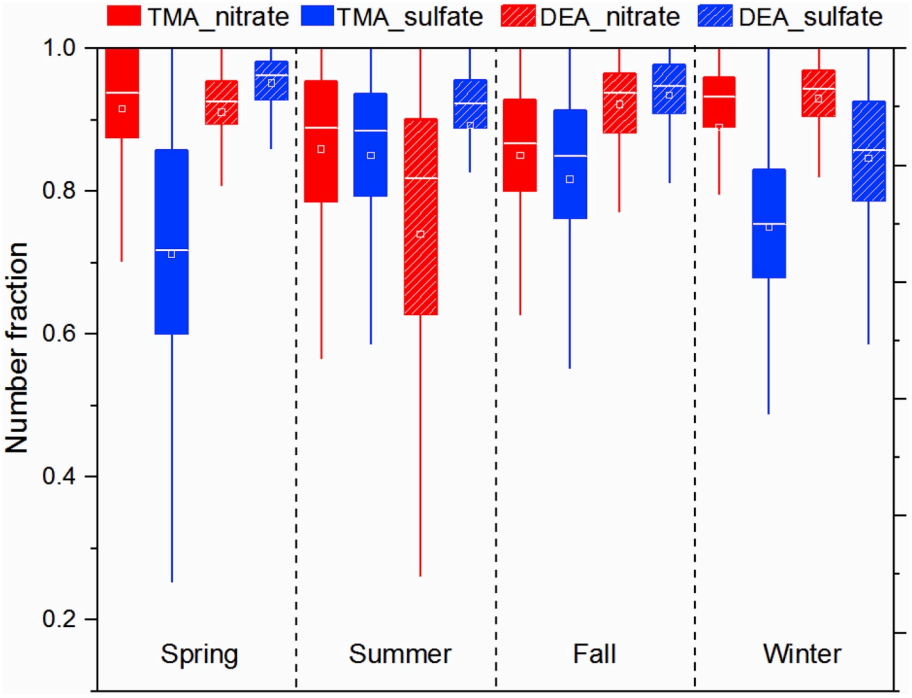

Fig. 3. Box plots of number fractions of nitrate and sulfate in DEA- and TMA-containing particles, respectively.

3.3. Mixing state of amine-containing particles

Amines are alkaline substances whose behavior is similar to that of ammonia; hence, it is expected to form aminium with sulfate or nitrate. Approximately 80% of amine-containing particles are found to be internally mixed with both nitrate and sulfate. This may be an indicative of sufficient atmospheric aging (Liu et al., 2003). In addition, strong correlations between the peak areas of DEA with sulfate ($r = 0.73–0.87$, $p < 0.01$) and nitrate ($r = 0.63–0.74$, $p < 0.01$), and those of TMA with nitrate ($r = 0.59–0.74$, $p < 0.01$) and sulfate ($r = 0.61–0.80$, $p < 0.01$) are observed in all seasons (Table S2). The peak area variation of different species detected by the SPAMS could be a good indicator for investigating the atmospheric process in individual particles (Chen et al., 2019; Cheng et al., 2018; Zhang et al., 2019). In the present study, the objective is not to reinforce the quantitative results, but to highlight the function of the most probable chemical form of amines. The strong correlations therefore support the existing chemical forms of amines, i.e., aminium sulfate and aminium nitrate.

Fig. 3 shows the box plots of number fractions of nitrate and sulfate in DEA- and TMA-containing particles, respectively. More amine-containing particles are mixed with sulfate in summer, but more are mixed with nitrate in winter. During spring and fall, amine-containing particles are similarly mixed with both nitrate and sulfate. It should be noted that the number fractions of sulfate in DEA-containing particles are observed to be higher than those in TMA-containing particles. This is consistent with the higher correlation between sulfate and DEA, rather than that between sulfate and TMA (Table S2). The stronger bond between sulfate and DEA could be attributed to different physicochemical properties of DEA and TMA. The acid solubility coefficient of DEA ($K_a = 1.45\times10^{-11}$ mol kg^{-1}) is one order of magnitude lower than that of TMA ($K_a = 1.58\times10^{-10}$ mol kg^{-1}) (Ge et al., 2011b). The vapor pressure of DEA sulfate ($p = 1.8\times10^{-12}$ Pa) at 298 K is three orders of magnitude lower than that of TMA sulfate ($p = 1.1\times10^{-9}$ Pa) (Lavi et al., 2013).

3.4. TMA oxidation

Previous laboratory studies have shown that amines can be oxidized by OH radical, NO_3 radical, and ozone, leading to formation of various compounds, such as trimethylamine oxide (TMAO), amides, N_2O, and HCN (Malloy et al., 2009; Murphy et al., 2007; Schade and Crutzen, 1995). With high level of oxidants in the atmosphere of the PRD region (Hofzumahaus et al., 2009), TMA may undergo oxidation to form TMAO. The marker ion for TMAO is identified as m/z 76 in a laboratory experiment (Angelino et al., 2001). In our observation, 8759 TMA-containing particles and 2793 TMAO-containing particles are obtained in the fall of 2013. The number fraction of TMAO-containing particles is 31.9% in the TMA-containing particles and only 2.5% in all detected particles. The number (in 3-h resolution) of TMA-containing particles is positively correlated with that of TMAO-containing particles ($r = 0.92$, $p < 0.01$). This confirms the assignment of m/z 76 to TMAO.

During this period, both TMA and TMAO-containing particles are classified into six types—OC–K, EC, Metal–rich, Dust, HMWOC, and Others by ART-2a followed by manual grouping (Section 2.3). The OC–K and HMWOC types account for 62.8% and 28.1% of TMAO-containing particles, respectively, significantly higher than those (43.4% and 12.0%) of TMA-containing particles (Fig. S3). A distinct feature of these two types is that they contain more oxidized organic species, such as formate (m/z −45 $[CHO_2]^-$), acetate (m/z −59 $[C_2H_3O_2]^-$), methylglyoxal or acrylate (m/z −71 $[C_3H_3O_2]^-$), and glyoxylate (m/z −73 $[C_3H_5O_2]^-$) (Zauscher et al., 2013; Zhang et al., 2019), than the other types (Fig. S4). These oxidized organics are generally formed through the photochemical oxidization of various volatile organic compounds (Zhang et al., 2019). The time series of the number fractions of the particles containing oxidized organics is correlated with that of the number fractions of TMAO-containing particles ($r = 0.28–0.40$, $p < 0.01$; Table S3) because of certain similarities in the oxidation process. One possible explanation for the higher association of HMWOC with TMAO-containing particles is that some HMWOC may be produced by the reactions between amines and these oxidized organics. A number of studies have reported that these oxidized organics can react with aliphatic amines to produce nitrogen-containing compounds with high molecular weight (De Haan et al., 2009; Powelson et al., 2014).

As shown in Fig. 4, the peak area ratios of TMAO and TMA in OC–K particles increase with the increasing RH, and decreasing O_3. These ratios, however, have no obvious relationship with the concentration of

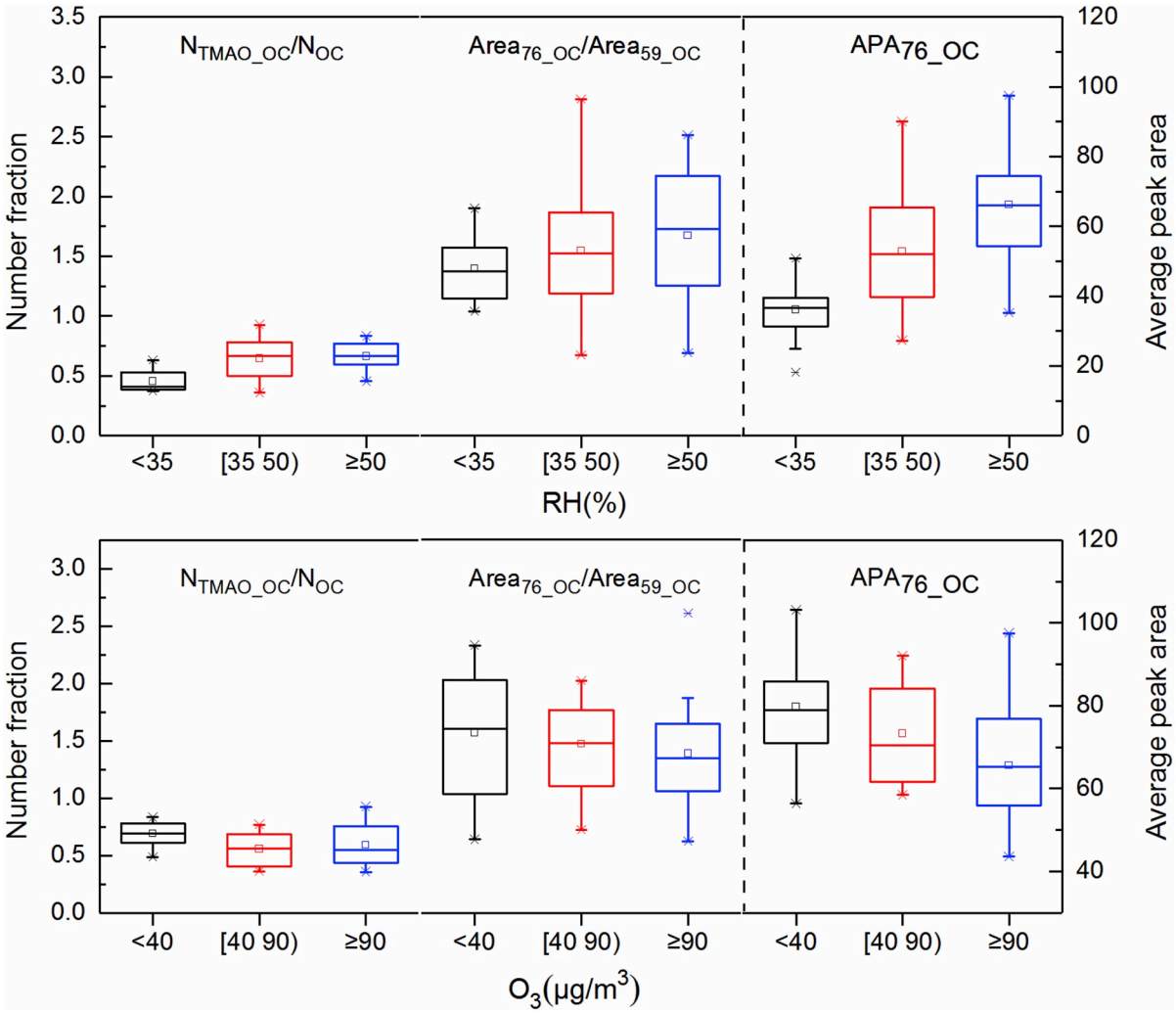

Fig. 4. Box plots of number fractions of TMAO (N_{TMAO_OC}/N_{OC}), peak area ratios of TMAO and TMA ($Area_{76\_OC}/Area_{59\_OC}$), and average peak areas of TMAO (APA_{76_OC}) in OC–K particles at different RH and ozone concentrations in fall of 2013.

other pollutants (SO_2, NO_X, and $PM_{2.5}$) and temperature (Fig. S5). The result indicates that TMAO is most probably produced through nighttime oxidation processes, rather than photochemical oxidation by O_3 and OH. Furthermore, the average peak area of TMAO is higher during nighttime (19:00–07:00) (Fig. S6), which is consistent with the diurnal variation of RH. Previous laboratory study shows that an increase of RH increases the yield of oxidation products in the reaction of amines with NO_3 radical, but have negligible effect on the aerosol yield through OH oxidation of amine (Tang et al., 2013). Regarding that NO_3 radical is an important oxidant of nighttime oxidation chemistry in the troposphere (Smith et al., 1995; Asaf et al., 2011), it is proposed that nighttime NO_3 oxidation may potentially contribute to the observed TMAO, however, contribution from other aqueous oxidations cannot be eliminated.

4. Conclusions

The seasonal variations of mixing state, evolution process, and influencing factors of amine-containing particles in the urban region of Guangzhou, China have been investigated. It is found that amine-containing particles are more abundant in spring and summer than in fall and winter. Their mass spectral patterns are clustered into eight types: OCEC, OC–K, EC, Metal–rich, Dust, NaK–EC, Amine–rich, and HMWOC. DEA and TMA are found to be the most ubiquitous and abundant in all seasons and are generally present in the form of aminium nitrate and/or aminium sulfate. The behaviors of DEA and TMA differ because they have different physicochemical properties. Compared with TMA, DEA is associated with more sulfate. It is also found that a large portion of TMA is oxidized to form TMAO, mainly through aqueous oxidation or NO_3 radical oxidation at nighttime, rather than oxidation by O_3. The results obtained herein provide insight into the mixing state and evolution of amines in the atmosphere.

Declaration of competing interest

The authors declare that they have no known competing financial interests or personal relationships that could have appeared to influence the work reported in this paper.

Acknowledgments

This work was jointly funded by the National Nature Science Foundation of China (No. 91544101, 41775124 and 41877307), the National Key Research and Development Program of China (No. 2017YFC0210104), the Science and Technology Project of Guangzhou, China (No. 201803030032), and the Guangdong Foundation for Program of Science and Technology Research (No. 2017B030314057). This is contribution from CASGIG NO. 2769.

Appendix A. Supplementary data

Supplementary data to this article can be found online at https://doi.org/10.1016/j.atmosenv.2019.117102.

References

Almeida, J., Schobesberger, S., Kürten, A., Ortega, I.K., Kupiainen-Määttä, O., Praplan, A. P., Adamov, A., Amorim, A., Bianchi, F., Breitenlechner, M., David, A., Dommen, J., Donahue, N.M., Downard, A., Dunne, E., Duplissy, J., Ehrhart, S., Flagan, R.C., Franchin, A., Guida, R., Hakala, J., Hansel, A., Heinritzi, M., Henschel, H., Jokinen, T., Junninen, H., Kajos, M., Kangasluoma, J., Keskinen, H., Kupc, A., Kurtén, T., Kvashin, A.N., Laaksonen, A., Lehtipalo, K., Leiminger, M., Leppä, J., Loukonen, V., Makhmutov, V., Mathot, S., McGrath, M.J., Nieminen, T., Olenius, T., Onnela, A., Petäjä, T., Riccobono, F., Riipinen, I., Rissanen, M., Rondo, L., Ruuskanen, T., Santos, F.D., Sarnela, N., Schallhart, S., Schnitzhofer, R., Seinfeld, J. H., Simon, M., Sipilä, M., Stozhkov, Y., Stratmann, F., Tomé, A., Tröstl, J., Tsagkogeorgas, G., Vaattovaara, P., Viisanen, Y., Virtanen, A., Vrtala, A., Wagner, P. E., Weingartner, E., Wex, H., Williamson, C., Wimmer, D., Ye, P., Yli-Juuti, T., Carslaw, K.S., Kulmala, M., Curtius, J., Baltensperger, U., Worsnop, D.R., Vehkamäki, H., Kirkby, J., 2013. Molecular understanding of sulphuric acid–amine particle nucleation in the atmosphere. Nature 502, 359–363.

Angelino, S., Suess, D.T., Prather, K.A., 2001. Formation of aerosol particles from reactions of secondary and tertiary alkylamines: characterization by aerosol time-of-flight mass spectrometry. Environ. Sci. Technol. 35, 3130–3138.

Asaf, D., Tas, E., Pedersen, D., Peleg, M., Luria, M., 2011. Long-term measurements of NO_3 radical at a semiarid urban site: 2. Seasonal trends and loss mechanisms. Environ. Sci. Technol. 44, 5901–5907.

Bi, X., Zhang, G., Li, L., Wang, X., Li, M., Sheng, G., Fu, J., Zhou, Z., 2011. Mixing state of biomass burning particles by single particle aerosol mass spectrometer in the urban area of PRD, China. Atmos. Environ. 45, 3447–3453.

Bzdek, B.R., Ridge, D.P., Johnston, M.V., 2010. Amine exchange into ammonium bisulfate and ammonium nitrate nuclei. Atmos. Chem. Phys. 10, 45–68.

Chen, Y., Tian, M., Huang, R.J., Shi, G., Wang, H., Peng, C., Cao, J., Wang, Q., Zhang, S., Guo, D., Zhang, L., Yang, F., 2019. Characterization of urban amine-containing particles in southwestern China: seasonal variation, source, and processing. Atmos. Chem. Phys. 19, 3245–3255.

Cheng, C., Huang, Z., Chan, C.K., Chu, Y., Li, M., Zhang, T., Ou, Y., Chen, D., Cheng, P., Li, L., 2018. Characteristics and mixing state of amine-containing particles at a rural site in the Pearl River Delta, China. Atmos. Chem. Phys. 18, 1–25.

De Haan, D.O., Corrigan, A.L., Smith, K.W., Stroik, D.R., Turley, J.J., Lee, F.E., Tolbert, M.A., Jimenez, J.L., Cordova, K.E., Ferrell, G.R., 2009. Secondary organic aerosol-forming reactions of glyoxal with amino acids. Environ. Sci. Technol. 43, 2818–2824.

De Haan, D.O., Hawkins, L.N., Welsh, H.G., Pednekar, R., Casar, J.R., Pennington, E.A., De, L.A., Jimenez, N.G., Symons, M.A., Zauscher, M.D., 2017. Brown carbon production in ammonium- or amine-containing aerosol particles by reactive uptake of methylglyoxal and photolytic cloud cycling. Environ. Sci. Technol. 51, 7458–7466.

Denkenberger, K.A., Moffet, R.C., Holecek, J.C., Rebotier, T.P., Prather, K.A., 2007. Real-time, single-particle measurements of oligomers in aged ambient aerosol particles. Environ. Sci. Technol. 41, 5439–5446.

Facchini, M.C., Decesari, S., Rinaldi, M., Carbone, C., Finessi, E., Mircea, M., Fuzzi, S., Moretti, F., Tagliavini, E., Ceburnis, D., 2008. Important source of marine secondary organic aerosol from biogenic amines. Environ. Sci. Technol. 42, 9116–9121.

Ge, X., Wexler, A.S., Clegg, S.L., 2011a. Atmospheric amines – Part I. A review. Atmos. Environ. 45, 524–546.

Ge, X., Wexler, A.S., Clegg, S.L., 2011b. Atmospheric amines – Part II. Thermodynamic properties and gas/particle partitioning. Atmos. Environ. 45, 561–577.

Healy, R.M., Evans, G.J., Murphy, M., Sierau, B., Arndt, J., Mcgillicuddy, E., O'Connor, I. P., Sodeau, J.R., Wenger, J.C., 2015. Single-particle speciation of alkylamines in ambient aerosol at five European sites. Anal. Bioanal. Chem. 407, 5899–5909.

Hofzumahaus, A., Rohrer, F., Lu, K., Bohn, B., Brauers, T., Chang, C.-C., Fuchs, H., Holland, F., Kita, K., Kondo, Y., Li, X., Lou, S., Shao, M., Zeng, L., Wahner, A., Zhang, Y., 2009. Amplified trace gas removal in the troposphere. Science 324, 1702–1704.

Huang, Y., Chen, H., Wang, L., Yang, X., Chen, J., 2012. Single particle analysis of amines in ambient aerosol in Shanghai. Environ. Chem. 9, 202–210.

Lavi, A., Bluvshtein, N., Segre, E., Segev, L., Flores, M., Rudich, Y., 2013. Thermochemical, cloud condensation nucleation ability, and optical properties of alkyl aminium sulfate aerosols. J. Phys. Chem. C 117, 22412–22421.

Li, L., Huang, Z., Dong, J., Li, M., Gao, W., Nian, H., Fu, Z., Zhang, G., Bi, X., Cheng, P., 2011. Real time bipolar time-of-flight mass spectrometer for analyzing single aerosol particles. Int. J. Mass Spectrom. 303, 118–124.

Liu, D.Y., Wenzel, R.J., Prather, K.A., 2003. Aerosol time-of-flight mass spectrometry during the Atlanta supersite experiment: 1. Measurements. J. Geophys. Res. 108, 8426.

Liu, F., Bi, X., Zhang, G., Lian, X., Fu, Y., Yang, Y., Lin, Q., Jiang, F., Wang, X., Peng, P.A., 2018. Gas-to-particle partitioning of atmospheric amines observed at a mountain site in southern China. Atmos. Environ. 195, 1–11.

Liu, F., Bi, X., Zhang, G., Peng, L., Lian, X., Lu, H., Fu, Y., Wang, X., Peng, P.A., Sheng, G., 2017. Concentration, size distribution and dry deposition of amines in atmospheric particles of urban Guangzhou, China. Atmos. Environ. 171, 279–288.

Müller, C., Iinuma, Y., Karstensen, J., Pinxteren, D.V., Lehmann, S., Gnauk, T., Herrmann, H., 2009. Seasonal variation of aliphatic amines in marine sub-micrometer particles at the Cape Verde islands. Atmos. Chem. Phys. 9, 9587–9597.

Malloy, Q.G.J., Li, Q., Warren, B., Cocker Iii, D.R., Erupe, M.E., Silva, P.J., 2009. Secondary organic aerosol formation from primary aliphatic amines with NO_3 radical. Atmos. Chem. Phys. 9, 2051–2060.

Marrero-Ortiz, W., Hu, M., Du, Z., Ji, Y., Wang, Y., Guo, S., Lin, Y., Gomez-Hermandez, M., Peng, J., Li, Y., Secrest, J., Zamora, M.L., Wang, Y., An, T., Zhang, R., 2019. formation and optical properties of Brown carbon from small alpha-dicarbonyls and amines. Environ. Sci. Technol. 53, 117–126.

Murphy, S.M., Sorooshian, A., Kroll, J.H., Ng, N.L., 2007. Secondary aerosol formation from atmospheric reactions of aliphatic amines. Atmos. Chem. Phys. 7, 2313–2337.

Pathak, R.K., Wu, W.S., Wang, T., 2009. Summertime $PM_{2.5}$ ionic species in four major cities of China: nitrate formation in an ammonia-deficient atmosphere. Atmos. Chem. Phys. 9, 1711–1722.

Powelson, M.H., Espelien, B.M., Hawkins, L.N., Galloway, M.M., De Haan, D.O., 2014. Brown carbon formation by aqueous-phase carbonyl compound reactions with amines and ammonium sulfate. Environ. Sci. Technol. 48, 985–993.

Pratt, K.A., Hatch, L.E., Prather, K.A., 2009. Seasonal volatility dependence of ambient particle phase amines. Environ. Sci. Technol. 43, 5276–5281.

Price, D.J., Clark, C.H., Tang, X., Cocker, D.R., Purvis-Roberts, K.L., Silva, P.J., 2014. Proposed chemical mechanisms leading to secondary organic aerosol in the reactions of aliphatic amines with hydroxyl and nitrate radicals. Atmos. Environ. 96, 135–144.

Qin, X., Prather, K.A., 2006. Impact of biomass emissions on particle chemistry during the California regional particulate air quality study. Int. J. Mass Spectrom. 258, 142–150.

Qiu, C., Zhang, R., 2013. Multiphase chemistry of atmospheric amines. Phys. Chem. Chem. Phys. 15, 5738–5752.

Rappert, S., Müller, R., 2005. Odor compounds in waste gas emissions from agricultural operations and food industries. Waste Manag. 25, 887–907.

Rehbein, P.J.G., Jeong, C.H., Mcguire, M.L., Yao, X., Corbin, J.C., Evans, G.J., 2011. Cloud and fog processing enhanced gas-to-particle partitioning of trimethylamine. Environ. Sci. Technol. 45, 4346–4352.

Rui, D.A., Bruns, R.E., Nobrega, R.P., 2009. Emission of polycyclic aromatic hydrocarbons from gasohol and ethanol vehicles. Atmos. Environ. 43, 648–654.

Schade, G.W., Crutzen, P.J., 1995. Emission of aliphatic amines from animal husbandry and their reactions: potential source of N_2O and HCN. J. Atmos. Chem. 22, 319–346.

Silva, P.J., Erupe, M.E., Price, D., Elias, J., Malloy, Q.G.J., Li, Q., Warren, B., Iii, D.R.C., 2008. Trimethylamine as precursor to secondary organic aerosol formation via nitrate radical reaction in the atmosphere. Environ. Sci. Technol. 42, 4689–4696.

Smith, N., Plane, J.M.C., Nien, C.F., Solomon, P.A., 1995. Nighttime radical chemistry in the san Joaquin valley. Atmos. Environ. 29, 2887–2897.

Song, X.H., Hopke, P.K., And, D.P.F., Prather, K.A., 1999. Classification of single particles analyzed by ATOFMS using an artificial neural network, ART-2a. Anal. Chem. 71, 860–865.

Sorooshian, A., Ng, N.L., Chan, A.W.H., Feingold, G., Flagan, R.C., Seinfeld, J.H., 2007. Particulate organic acids and overall water-soluble aerosol composition measurements from the 2006 Gulf of Mexico Atmospheric Composition and Climate Study (GoMACCS). J. Geophys. Res. Atmos. 112, D13201.

Tang, X., Price, D., Praske, E., Su, A.L., Shattuck, M.A., Purvis-Roberts, K., Silva, P.J., Asa-Awuku, A., Iii, D.R.C., 2013. NO_3 radical, OH radical and O_3-initiated secondary aerosol formation from aliphatic amines. Atmos. Environ. 72, 105–112.

Tao, J., Shen, Z., Zhu, C., Yue, J., Cao, J., Liu, S., Zhu, L., Zhang, R., 2012. Seasonal variations and chemical characteristics of sub-micrometer particles (PM_1) in Guangzhou, China. Atmos. Res. 118, 222–231.

Youn, J.S., Crosbie, E., Maudlin, L.C., Wang, Z., Sorooshian, A., 2015. Dimethylamine as a major alkyl amine species in particles and cloud water: observations in semi-arid and coastal regions. Atmos. Environ. 122, 250–258.

Zauscher, M.D., Ying, W., Moore, M.J.K., Gaston, C.J., Prather, K.A., 2013. Air quality impact and physicochemical aging of biomass burning aerosols during the 2007 San Diego wildfires. Environ. Sci. Technol. 47, 7633–7643.

Zhang, G., Bi, X., Chan, L.Y., Li, L., Wang, X., Feng, J., Sheng, G., Fu, J., Li, M., Zhou, Z., 2012. Enhanced trimethylamine-containing particles during fog events detected by single particle aerosol mass spectrometry in urban Guangzhou, China. Atmos. Environ. 55, 121–126.

Zhang, G., Han, B., Bi, X., Dai, S., Huang, W., Chen, D., Wang, X., Sheng, G., Fu, J., Zhou, Z., 2015. Characteristics of individual particles in the atmosphere of Guangzhou by single particle mass spectrometry. Atmos. Res. 153, 286–295.

Zhang, G., Lin, Q., Peng, L., Yang, Y., Jiang, F., Liu, F., Song, W., Chen, D., Cai, Z., Bi, X., 2019. Oxalate formation enhanced by Fe-containing particles and environmental implications. Environ. Sci. Technol. 53, 1269–1277.